INSTITUTE OF PHYSICS PUBLISHING JOURNAL OF PHYSICS B: ATOMIC, MOLECULAR AND OPTICAL PHYSICS

J. Phys. B: At. Mol. Opt. Phys. **36** (2003) 1029–1039 PII: S0953-4075(03)56542-7

Prospects for the creation of positron–electron plasmas in a non-neutral stellarator

T Sunn Pedersen[1], **A H Boozer**[1], **W Dorland**[2], **J P Kremer**[1] **and R Schmitt**[1]

[1] Department of Applied Physics and Applied Mathematics, Columbia University, NY 10027, USA
[2] Department of Physics, University of Maryland, College Park, MD 20742, USA

E-mail: tsp22@columbia.edu

Received 22 November 2002
Published 24 February 2003
Online at stacks.iop.org/JPhysB/36/1029

Abstract

The prospects of creating positron–electron plasmas confined in a stellarator are discussed. A pure electron plasma would be created before the positrons are introduced, to facilitate efficient injection and a long confinement time of the positrons. Gyrokinetic simulations are presented suggesting that a positron–electron plasma may be stable to low-frequency microturbulence if operated well below the Brillouin limit, and transport may be neoclassical. If this is the case, significant positron–electron plasma densities can be reached with positron sources that exist today.

1. Introduction

Toroidal magnetic surface configurations, most notably the tokamak and the stellarator, are the most successful confinement devices for fusion plasmas. Until recently, this family of confinement devices had not been used to confine non-neutral plasmas, but now there is a levitated ring trap, the prototype-ring trap [1], being used for pure electron plasma confinement, and a stellarator, the Columbia non-neutral torus (CNT), being constructed to study pure electron and partly neutralized plasmas [2]. A stellarator is a magnetic surface configuration created entirely from external coils with no need for a plasma current or conductors inside the plasma [3]. Stellarators have important advantages for the creation of the first confined laboratory positron–electron plasmas, namely the ability to confine positrons and electrons simultaneously in the same volume, at any degree of neutrality and at relatively high particle kinetic energies, the ability to operate steady state, and the ability to operate at ultralow densities. In this paper, we discuss some important criteria for the success of a confined positron–electron plasma experiment. We present and analyse a two-step process of creating positron–electron plasmas in a stellarator. The first step would be the creation of a pure electron plasma with $a/\lambda_D \gg 1$ in the stellarator. Here, λ_D is the electron Debye length,

0953-4075/03/051029+11$30.00

$\lambda_D^2 = \epsilon_0 T_e/(ne^2)$. This step will be addressed in the CNT experiment. For the purposes of this paper, we assume that this step is achievable [2]. The second step is the injection of the positrons, which will be confined not only by the magnetic field but also by the space charge of the electrons, which provides a force on the positrons pulling them towards the plasma centre. We show that the collisional confinement would allow for the successful creation of confined positron–electron plasmas with realistic positron sources. However, if the plasma becomes turbulent, the confinement time will not be sufficient to guarantee significant accumulation of positrons in the trap. We have begun to investigate the microstability of positron–electron plasmas in toroidal magnetic configurations using the gyrokinetic simulation code GS2. We present initial simulations in an axisymmetric (tokamak) configuration that show that the plasma will be stable to low-frequency ($\omega \ll eB/m_e$) waves if the plasma density is well below the Brillouin density $n_e \ll n_B = \epsilon_0 B^2/(2m_e)$ [4]. Above the Brillouin density, we observe an interchange instability which causes significant transport. If these results carry over to a non-axisymmetric (stellarator) configuration, turbulent transport will not prevent the success of the proposed approach to creation of laboratory positron–electron plasmas.

2. Properties and importance of positron–electron plasmas

Positron–electron plasmas are unique because of their perfect symmetry of mass and perfect antisymmetry of charge. The perfect symmetry of quasi-neutral, equal temperature positron–electron plasmas makes them the simplest possible quasi-neutral plasmas that one can study analytically or numerically. The symmetry directly eliminates certain wave types, such as (ion) acoustic waves, and consequently electrostatic drift waves [5]. Since the two species evolve on the same spatial and temporal scales, accurate numerical simulations are easier to perform for pair plasmas than for ion–electron plasmas.

The creation of a confined positron–electron plasma is an experimental challenge that has not yet been met because of the relative weakness of available positron sources (as compared with electron or ion sources). Hence, a comparison of theoretical and numerical predictions with a confined positron–electron experiment has not yet been performed, although it would clearly benefit our understanding of basic plasma physics significantly. The most significant experimental achievements towards this goal are the studies of positron plasmas interacting with electron beams [6], which were in good agreement with theoretical predictions.

Positron–electron plasmas are also thought to be important in a number of astrophysical phenomena (see e.g. [7–9]), and this provides additional motivation for understanding the dynamics of these plasmas better.

The study of positron–electron plasmas would also have an impact on fusion science. Hot magnetized electron–ion plasmas have been studied intensely in magnetic fusion research for 50 years, and it has become clear that the behaviour of these plasmas is far more complex than was anticipated in the early days of plasma fusion research. Transport of particles and heat across the magnetic field occurs much more rapidly than can be accounted for by collisional processes. The cross-field transport is dominated by turbulent mixing of the plasma across the magnetic field lines, caused by waves that are unstable on small spatial scales, such as electrostatic drift waves. These effects are clearly seen in numerical simulations, and good agreement has been found between experiments and simulations. However, it is not clear that these simulation models capture the basic physics accurately enough to predict the turbulent transport of future fusion reactor devices. A positron–electron experiment would provide a way to validate the physics capabilities of physics transport codes, since at least some of these codes, e.g. the GS2 code used in this paper, can be made to simulate positron–electron plasmas rather easily, including the effects of magnetic geometry such as curvature and shear.

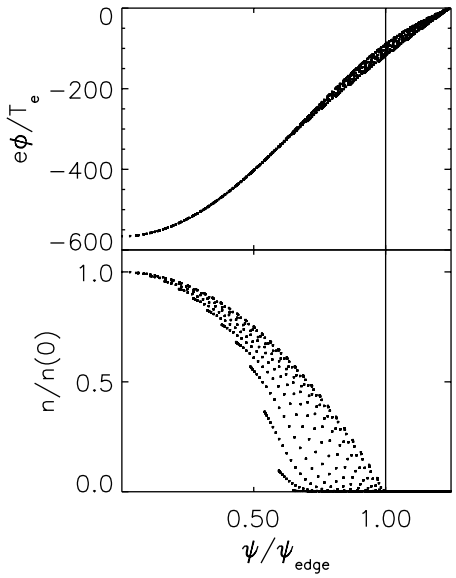

Figure 1. Scatter plots of n_e and $e\phi/T_e$ plotted versus the magnetic surface variable ψ.

3. Equilibrium of a single-component plasma

The equilibrium equation of a low-density, $n_e \ll n_B = \epsilon_0 B^2/(2m_e)$ [4], pure electron plasma in a magnetic surface configuration is [2]:

$$\epsilon_0 \nabla^2 \phi = eN(\psi) \exp\left(\frac{e\phi}{T_e(\psi)}\right) \tag{1}$$

where ψ is a coordinate that labels the magnetic surface (i.e. each magnetic surface is described by ψ = constant), ϕ is the electrostatic potential and e is the unit charge. T_e is the electron temperature, which is assumed constant on a magnetic surface, but which may vary from surface to surface. $N(\psi)$ is a magnetic surface function that has units of density and is related to the actual density, which is generally not a magnetic surface function, through $n_e = N(\psi)\exp(e\phi/T_e(\psi))$. By replacing e with $-e$, one finds the equivalent pure positron plasma equilibrium equation. Numerical solutions of the equilibrium equation in two dimensions have recently been extended from the $a^2/\lambda_D^2 < 100$ regime reported earlier [10], to $a^2/\lambda_D^2 \approx 1000$. Here, a is the characteristic smallest dimension of the plasma. The equilibria studied here are on elliptical magnetic surfaces surrounded by a vacuum region and a perfect conductor that matches a vacuum magnetic surface. For these small Debye length plasmas, the density contours become more elongated than the magnetic surfaces, $b/a \approx 2.5$, whereas the magnetic surfaces have $b/a = \sqrt{3}$. In figure 1 we show the normalized equilibrium density n_e and electrostatic potential $e\phi/T_e$ as functions of the magnetic surface coordinate ψ. The vertical scatter in each plot indicates the degree to which the quantity varies on a magnetic surface. The electrostatic potential varies only slightly on a magnetic surface, although some scatter is evident in the outer parts of the plasma. The density varies strongly on a magnetic surface, particularly in the outer parts. However, the electrostatic potential is nearly constant on any part of the magnetic surface that has appreciable density. This is illustrated in figure 2, where we have excluded points that have a plasma density less than 10^{-3} of the central density. The total fraction of electrons excluded in this figure is only 5×10^{-5}.

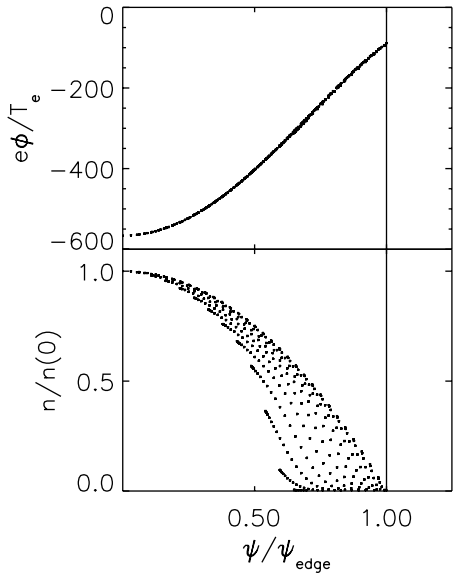

Figure 2. Scatter plots of n_e and $e\phi/T_e$ plotted versus the magnetic surface variable ψ, excluding all points where $n/n(0) < 10^{-3}$.

Calculation of these small Debye length equilibria were facilitated by elimination of round-off errors and numerical under- and overflow problems associated with the exponential factor, which varies by several hundreds of orders of magnitude over the computational domain when $a^2/\lambda_D^2 \approx 1000$. The most important change is to write the solution ϕ as the sum of a large and a small part, $\phi = \phi_0 + \phi_1$, and solve the following equation for ϕ_1:

$$\epsilon_0 \nabla^2 \phi_1 = e n_0 \exp\left(\frac{e\phi_1}{T_e}\right) - \epsilon_0 \nabla^2 \phi_0 \tag{2}$$

with $n_0 = N(\psi)\exp(e\phi_0/T_e)$. For any realistic density, n_0 is a well-behaved function, since it approximates the density well, as long as $e\phi_1/T_e$ is of order 1 or less. This is true even if $N(\psi)$ and $\exp(e\phi_0/T_e)$ separately vary by hundreds of orders of magnitude. Equation (2) is solved iteratively using the same technique that was used to solve equation (1) [10]. The initial ϕ_0 is supplied by solving equation (1) iteratively until numerical problems arise. If the iterative solution for ϕ_1 grows large (because ϕ_0 is not close enough to the actual solution of the equation), one simply redefines ϕ_0 as $\phi_0 + \phi_1$, recalculates n_0, and starts solving for a new ϕ_1 with the updated version of equation (2). This process may be repeated until the desired accuracy of the solution is obtained. The opposite limit, $a^2/\lambda_D^2 \ll 1$ is physically and computationally trivial; solutions are of the form $n_e = N(\psi)$, $|e\phi|/T_e \ll 1$ in this case.

4. Confinement time of single-component and partly neutralized plasmas

4.1. Confinement of single-component plasmas

The collisional particle confinement time of a pure electron plasma is approximately [2]:

$$\tau_p \approx \tau_e \frac{a^4}{\lambda_D^4}. \tag{3}$$

The physics behind this scaling is as follows: each time a particle suffers a collision, it takes a random step across the magnetic surfaces which is of the order of the deviation of the particle's guiding centre orbit from its magnetic surface. This type of transport is called neoclassical transport. The guiding centre deviations from a magnetic surface are caused by ∇B and curvature drifts, $\boldsymbol{v}_{\nabla B+R} = (mv_\parallel^2 + \frac{1}{2}mv_\perp^2)\nabla B \times \boldsymbol{B}/(eB^3)$, as well as $E \times B$ drifts, $\boldsymbol{v}_E = \boldsymbol{E} \times \boldsymbol{B}/B^2$. The former result in deviations from a magnetic surface which are proportional to $v_{\nabla B+R}/v_E \propto \lambda_D^2$, because the $\boldsymbol{v}_E$ in a non-neutral plasma usually provides an effective rotational transform of the guiding centres which exceeds that provided by the magnetic field. The $\boldsymbol{v}_E$ drift will tend to move the particle on a guiding centre orbit described by $\phi =$ constant, so to the extent that ϕ varies on a magnetic surface, the particle will experience excursions away from the magnetic surface that are proportional to $\delta\phi/\phi$. Parallel force balance between the gradient of the pressure $p = n_e T_e$ and the electric field force implies $\delta\phi \approx p/(en_e) = T_e/e$, so $\delta\phi/\phi \propto \lambda_D^2$. In a generic magnetic surface configuration, the two effects will be of the same order. However, it should be noted that careful tailoring of the magnetic field topology can reduce the $\boldsymbol{v}_{\nabla B+R}$ deviations from the magnetic surfaces by several orders of magnitude. Careful tailoring of the boundary conditions of ϕ outside the plasma can also reduce $\delta\phi/\phi$ significantly. Such an optimization would increase the confinement time predicted in equation (3) by a large factor.

We plan to study the transport of particles in more detail using a particle-following code.

4.2. Confinement of partly neutralized plasmas

When positrons are injected into an initially pure electron plasma, the confinement properties change. In this case, the Debye screening length λ_D is given by

$$\lambda_D^{-2} = \frac{e^2}{\epsilon_0}\left(\frac{n_e}{T_e} + \frac{n_p}{T_p}\right). \tag{4}$$

Hence, the addition of a finite positron density will decrease λ_D. At the same time, the space charge is reduced, so the electric field is reduced. The deviations from a magnetic surface due to $\boldsymbol{v}_{\nabla B+R}$ now scale with $\lambda_C^2 = \epsilon_0 T_e/(e^2|n_e - n_p|)$, a space charge Debye length, or 'Coulomb length'.

The existence of a positive species in addition to the negative species will allow the plasma to shield out parallel electric fields more efficiently, so $\delta\phi/\phi$ on each magnetic surface decreases significantly, and the $E \times B$ drift will no longer cause significant deviations of the particle guiding centres from the magnetic surfaces. Hence, the confinement of electrons is now given by:

$$\tau_p = \tau_e \frac{a^4}{\lambda_C^4}, \qquad \lambda_C^4 = \frac{(n_e + n_p)^2}{(n_e - n_p)^2}\lambda_D^4. \tag{5}$$

As long as $a/\lambda_C \gg 1$, positrons will be confined much better than the electrons, by the space charge potential in addition to the magnetic confinement.

Quasi-neutral ion–electron plasmas, which have $\lambda_D \ll \lambda_C$, usually develop an electrostatic potential $|\phi| \approx T/e$ where T is the temperature of one species, and the sign of ϕ is determined by the details of the experiment (usually negative in toroidal plasmas). This is the potential that develops to enforce ambipolar transport. Electrostatic fields of this order imply that a/λ_C is close to 1, so we would estimate $\tau_p \sim \tau_e$ for such plasmas. In a generic magnetic surface configuration without any symmetry, which is the basis of our transport estimate, the confinement time may only be of the order of the collision time. In stellarators optimized for neoclassical transport and in tokamaks (which have toroidal symmetry), much longer confinement times can be achieved even when $a/\lambda_C \sim 1$.

5. Gyrokinetic calculations

In toroidal fusion plasmas, transport is generally not neoclassical, but is dominated by turbulence driven by microinstabilities. We have begun to investigate the microstability of quasi-neutral positron–electron plasmas in toroidal magnetic configurations. Although drift waves and acoustic waves are not found in a pair plasma, it is not difficult to see that the basic curvature-driven interchange instability threatens confinement. Straightforward analysis shows that in the absence of magnetic shear, bad curvature induces an interchange in a pair plasma with a growth rate that scales like $\gamma \sim v_t/\sqrt{RL}$, where v_t is the thermal velocity, R is the radius of curvature and L is the characteristic pressure gradient scale length of the plasma; in the absence of other microinstabilities, the interchange is thus a strong candidate for driving turbulence in a laboratory pair plasma confined with a magnetic field. This instability is well-described by the gyrokinetic formalism [11, 12]. We use the GS2 nonlinear gyrokinetic code, which was developed and extensively benchmarked for fusion plasma turbulence studies [13, 14], to perform a numerical study of the microstability of toroidal pair plasmas. The GS2 code can be straightforwardly applied to pair plasmas by specifying the mass of the singly charged ions to be equal to the electron mass.

It is easy to demonstrate the lack of drift waves or the pair-plasma version of the sheared-slab η_i mode analytically and numerically. We have done this with GS2. The η_i mode is not expected to be unstable in a pair plasma because it is essentially a destabilized ion acoustic wave, which is not present in the laboratory pair plasma. Not all microinstabilities are thwarted by the mass symmetry, however. Here, we show that, in principle, observable gyrokinetic turbulence may be expected in a laboratory positron–electron plasma unless $n \ll n_B$, where n_B is the Brillouin density [4]. The pair plasma creation method outlined in section 7 would result in pair plasmas with $n \ll n_B$, and hence turbulence would not be observed in such plasmas. However, in principle $n \gg n_B$ pair plasmas could be created.

We consider the basic expectation for transport in a pair plasma that is unstable to the collisionless interchange, in an axisymmetric, circular flux surface, low-β (tokamak) configuration for which much numerical study has already been carried out [15]. In this case, the density gradient $R/L_n = 2.2$, the temperature gradient $R/L_T = 6.9$, the inverse aspect ratio $a/R = 0.36$, the safety factor $q = 1.4$, the magnetic shear $\hat{s} = 0.8$, $T_i = T_e$, and we are considering turbulent radial heat and particle flux through the surface at $r/a = 0.5$. For a conventional deuterium plasma, several benchmarked gyrokinetic simulation codes (including GS2) predict an ion energy diffusion coefficient in this case of $\chi_i = 0.8\rho_i^2 v_{ti}/L_T$. The instability which leads to this anomalous transport flux is the ion temperature gradient mode.

In a pair plasma with the same equilibrium characteristics, we find a much higher transport rate in units of $\rho^2 v_t/L_T$ for these parameters. In this case, the underlying instability is the short-wavelength interchange mode. The energy diffusion coefficient for each species is $\chi_i \sim 150\rho^2 v_t/L_T$. Additionally, we find a particle diffusion coefficient of $D \sim 50\rho^2 v_t/L_n$. The larger dimensionless transport is due to higher nonlinear saturation amplitudes of the turbulence. However, in physical units, the transport is only somewhat larger, since $\rho^2 v_t$ is $\sqrt{3672} \approx 60$ times smaller than that of a deuterium plasma with the same temperature. For realistic experimental values, the resulting transport rate would far exceed neoclassical transport, and one would not be able to reach or sustain any appreciable positron density with present positron sources. We have made no attempt at this point to optimize the configuration for interchange stability, nor have we investigated non-axisymmetric (stellarator) configurations, but we intend to do so in the future.

In figure 3, we show the maximum growth rate γ_{max} versus plasma density in an axisymmetric magnetic configuration which resembles a tokamak. This configuration has

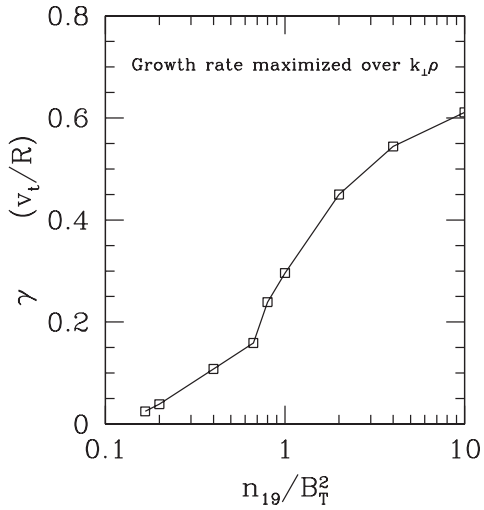

Figure 3. The growth rate of the most unstable mode versus normalized plasma density.

average good curvature and magnetic shear, both of which act to stabilize the interchange modes in conventional ion–electron plasmas (and similarly in the positron–electron plasma). The magnetic field $B_T = 1$ T, the gradients are taken to be $R/L_n = R/L_T = 3$, and the remaining parameters are similar to the case above. The growth rate is maximized over all $k_\perp \rho$. (The peak value tends to be around $k_\perp \rho \sim 0.2$.)

If the transport is large when the interchange mode is destabilized, then figure 3 indicates that there will be a maximum operating density. The physics behind the low-density cut-off is as follows: as the density is lowered, the Debye length approaches and eventually exceeds the thermal gyroradius. The key stability parameter is $(\rho/\lambda_D)^2 = 2n/n_B$ where n_B is the Brillouin density, $n_B = \epsilon_0 B^2/(2m_e)$ [4]. For low enough density, the positron–electron interchange instability is stabilized by the finite Debye length, at reasonable values of R/L_n. In the case studied, $n/n_B < 0.2$ is sufficient for stability, but in general, this ratio depends on R/L_n. Shorter density gradient scale lengths increase the maximum linear growth rate at fixed density, shift the low-density threshold to lower density and lower the range of $k_\perp \rho$ of the instability. That is, stable operation at steeper gradients requires a lower value of n/n_B. We compare the linear physics with results from conventional ion–electron plasmas by artificially varying the electron to ion mass ratio. In figure 4, the maximized growth rate (normalized by v_{ti}/R) is plotted against ratio of electron mass to ion mass. Conventional plasma mass ratios correspond to the left side of the figure, and the pair plasma is at unity on the x-axis, where $m_e = m_i$. The apparent asymmetry of the growth rate is due to its normalization to v_{ti}. Here, we have taken the density to be high enough, $n \gg n_B$, that Debye screening is unimportant. The unique instability of the pair plasma is evident as the mass ratios become more similar.

6. Requirements for laboratory positron–electron plasma experiments

The most fundamental requirement for the success of any positron–electron plasma physics experiment is to simultaneously confine several Debye lengths of each species in the same volume:

$$\lambda_{De}^2 = \epsilon_0 T_e/(n_e e^2) \ll a^2, \qquad \lambda_{Dp}^2 = \epsilon_0 T_p/(n_p e^2) \ll a^2. \tag{6}$$

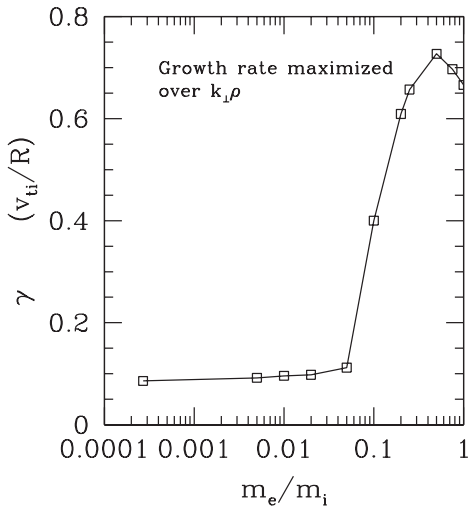

Figure 4. The maximized growth rate is plotted as a function of the mass ratio, as calculated by the gyrokinetic code GS2.

This is a challenge because available positron sources are weak compared with the plasma particle sources that are usually used in experiments. If we require the positrons to be relatively cold, which favours a small Debye length and may increase confinement time and decrease ionization of neutrals in the trap, the source rates drop off more dramatically. Available positron sources are many orders of magnitude weaker than those of electrons. The most intense continuous sources of relatively cold positrons, $T_p \sim 3$ eV, are, to the best of our knowledge, in the range of 10^8 positrons s^{-1} [16], with sources of 10^9 positrons s^{-1} expected to be available in the near future [16, 17]. By comparison, 1 cm^2 of thoriated tungsten wire can thermionically emit of the order of 10^{19} electrons s^{-1} with $T_e < 1$ eV. In the future, arrays of high-field Penning traps may be able to store as many as 10^{12} positrons [20]. Such a large nearly instantaneous source of cold positrons would make a positron–electron plasma experiment highly likely to succeed. Our discussion here will focus on the more challenging task of creating a positron–electron plasma using continuous sources of cold positrons at the level reached today ($S = 10^8$ s^{-1}) or projected for the near future ($S = 10^9$ s^{-1}).

7. A method for creation of positron–electron plasmas

In order to accumulate sufficient amounts of cold positrons to satisfy $\lambda_{Dp} \ll a$, confinement must be excellent. This has been achieved in Penning traps [18] in several experiments, but Penning traps cannot simultaneously confine positive and negative species. In a nested Penning trap [19], one can simultaneously confine the two species in adjacent traps, which can be arranged such that the two species overlap spatially, since the most energetic particles of one species can climb the potential that is used to confine the other species. However, it can be shown that the criterion in equation (6) cannot be satisfied in such a trap.

Stellarators trivially confine both species in the same volume. This is also true for the magnetic mirror [5] and a combined Penning–Paul trap [20], both of which are potential candidates for a positron–electron plasma confinement scheme. By comparison, the stellarator will have much better confinement than a magnetic mirror, and can confine many more energetic particles and much larger space charges than the Penning–Paul trap. The potentially low

confinement time in a stellarator is a serious concern though. However, when $\lambda_C \ll a$, the confinement time can be very long for both species, in particular the one that is the minority species. Given the large difference in available sources for electrons and positrons, it is obvious that one would want to operate with a surplus of electrons. Specifically, we will consider a scenario where a pure electron plasma with $a/\lambda_{De} \gg 1$ has already been created. Such a plasma will necessarily have $n_e < n_B$. The method of creation of such plasmas will be a near-term goal of the CNT experiment. For the purposes of this paper, we assume that this goal has been successfully achieved and do not discuss it further. It may be possible to have internal steady state sources of electrons, but we will show in the following that even without such sources, one can successfully create positron–electron plasmas.

Once a pure electron plasma is created, and the plasma is separated from any electron-emitting filaments, the positrons are injected from the edge. Pulled by the electrostatic potential of the electrons, the positrons will diffuse inward through the same neoclassical transport processes that make the electrons diffuse out. As long as the electrostatic field is strong enough that $-e\phi/T_p \gg 1$, the positrons will be very well trapped. As the positrons accumulate, a quasi-neutral region will start to grow starting at the plasma centre, surrounded by an electron-rich region which the positrons continue to diffuse through. However, as the positrons accumulate, the confinement time of the electron plasma decreases because of the neutralization. Unless electrons can also be simultaneously injected, the entire plasma will decay away on the time scale given by equation (5). We now estimate the peak positron density during this second phase, ignoring profile effects, which would require a much more detailed calculation. Since $n_e < n_B$, we expect the interchange mode seen in our gyrokinetic simulations to be stable, and that transport therefore is neoclassical. We assume that, at the point where the positron density peaks, the positron confinement time is equal to the electron confinement time, so that $S = V n_p^{max}/\tau_p$, with τ_p given by equation (5). This is clearly very conservative, but it guarantees that the positrons have had time to accumulate before the initial electron density has decayed more than one e-folding time, τ_p, and that the positrons have had one inward diffusion time (also τ_p) to diffuse to the centre of the electron plasma. Expressing the plasma volume as $V = 2\pi^2 a^2 R$, where a is an effective minor radius and R is an effective major radius, $1/\tau_e = \sqrt{2} n_e e^4 \ln\Lambda/(12\pi^{3/2}\epsilon_0^2\sqrt{m_e}T^{3/2})$, we arrive at the following relation:

$$\frac{n_e n_p^{max}}{(n_e - n_p^{max})^2} = \frac{6a^2}{\sqrt{2\pi}\ln\Lambda R v_{th}} S \equiv \tilde{S}. \tag{7}$$

Here, $v_{th} = \sqrt{T/m_e}$. When $\tilde{S} \gg 1$, $n_p \approx n_e$, and the plasma reaches close to charge neutrality. When $\tilde{S} \ll 1$, $n_p \approx \tilde{S} n_e$. It is encouraging that $\tilde{S} > 1$ for realistic parameters. For example, $T_e = 1$ eV, $S = 10^9$ s^{-1}, $a = 0.1$ m, $R = 0.3$ m, $\ln\Lambda = 15$ yields $\tilde{S} = 12$. For currently available sources, $S = 10^8$ s^{-1}, $\tilde{S} = 1.2$. The peak positron density can therefore be expected to be a significant fraction of the initial electron density. Thus, one will want to maximize the initial density of the pure electron plasma, or more specifically, maximize the number of electron Debye lengths. If $\tilde{S}$ is of order 1 or larger, the number of positron Debye lengths at peak density will be about three times smaller than the initial electron density, and therefore, if the initial pure electron plasma has $a/\lambda_{De} \gg 1$, $a/\lambda_{De} \gg 1$ and $a\lambda_{Dp} \gg 1$ will be simultaneously achieved after about one electron plasma confinement time.

8. Other experimental concerns

In addition to having excellent positron confinement, there are several other requirements that must be met by any positron–electron plasma experiment, regardless of the particular

confinement method, in order to create an uncontaminated positron–electron plasma. Some of these have been considered in previous publications on this topic [20].

8.1. Ion contamination

Neutral atoms may become ionized in the plasma, and the resulting positive ions will become trapped by the electric potential just as the positrons. One may be able to tolerate a small fraction of ions without changing the dynamics of the positron–electron plasma significantly, but if the goal is to study electron–positron plasmas, then the ion fraction must not be large. Hence, the source rate of ions must be much less than the source rate of positrons:

$$S \gg V n_n n_e \langle \sigma v \rangle \tag{8}$$

with n_n being the neutral density, V the plasma volume and $\langle \sigma v \rangle$ the rate coefficient for collisional ionization. If equation (8) is satisfied, then ions will not significantly contaminate the positron–electron plasma. We estimate the severity of this constraint by assuming that the neutrals consist of atomic hydrogen at room temperature, and that the plasma has dimensions $R = 0.3$ m, $a = 0.1$ m, density $n_e = 10^{13}$ m^{-3}, and the source rate of positrons is 10^9 s^{-1}. The required vacuum neutral pressure p_n is a strong function of temperature [21]. At $T_e = 1$ eV, $p_n \ll 4.6 \times 10^{-6}$ Torr. At 2 eV, $p_n \ll 3.7 \times 10^{-9}$ Torr. For $T_e > 5$ eV, the temperature becomes less important and $p_n \ll 10^{-12}$ Torr is required. Although this constraint is non-trivial, there are numerous non-neutral plasma experiments that operate in a regime where equation (8) is satisfied, partly because significant ionization leads to an uncontrolled, and usually undesirable, density rise in Penning trap pure electron experiments, so care is taken to avoid it.

8.2. Positron annihilation on plasma electrons and neutrals

In addition to diffusion, other positron loss mechanisms may be important. Annihilation on plasma electrons is only significant if low temperatures and relatively high densities are achieved. For example, if $T_p = T_e = 1$ eV and $n_e \approx n_p = 10^{13}$ m^{-3} in an $R = 0.3$ m, $a = 0.1$ m stellarator, there will be $\sim 5 \times 10^6$ annihilations s^{-1} [22], still orders of magnitude less than source rates of 10^8–10^9 positrons s^{-1}, but plenty to make annihilation gamma-ray detection a potentially useful diagnostic. Positrons may also annihilate on neutral atoms, but this loss mechanism is negligibly small at $p_n < 10^{-9}$ Torr, as long as the trap is free of hydrocarbons [20].

9. Future work

Confinement of pure electron plasmas will be studied experimentally in the CNT device being constructed at Columbia University. If this experiment succeeds in producing $a \gg \lambda_{De}$ pure electron plasmas with confinement $\tau_p \approx \tau_e (a/\lambda_{De})^4$, then $a \gg \lambda_{De}$ and $a \gg \lambda_{Dp}$ can be simultaneously reached even with rather modest positron sources in a similar stellarator experiment devoted to positron–electron plasma physics. A conceptual, optimized design of such an experiment can be made on the basis of the requirements and tools described here.

References

[1] Yoshida Z *et al* 1999 *Non-Neutral Plasma Physics III (AIP Conf. Proc. vol 498)* (New York: American Institute of Physics) p 397

[2] Sunn Pedersen T and Boozer A H 2002 *Phys. Rev. Lett.* **88** 205002

[3] Boozer A H 1998 *Phys. Plasmas* **5** 1647
[4] Brillouin L 1945 *Phys. Rev.* **67** 260
[5] Tsytovich V and Wharton C B 1978 *Comment. Plasma Phys. Control. Fusion* **4** 91
[6] Greaves R G and Surko C S 1995 *Phys. Rev. Lett.* **75** 3846
[7] Wardle J F C, Homan D C, Ojha R and Roberts D H 1998 *Nature* **395** 457
[8] Rees M J 1971 *Nature* **229** 312
[9] Mofiz U A 1992 *Astrophys. Space Sci.* **196** 101
[10] Sunn Pedersen T 2003 *Phys. Plasmas* **10** 334
[11] Frieman E A and Chen L 1982 *Phys. Fluids* **25** 502
[12] Antonsen T and Lane B 1980 *Phys. Fluids* **23** 1205
[13] Kotschenreuther M, Rewoldt G and Tang W M 1995 *Comput. Phys. Commun.* **88** 128
[14] Dorland W, Jenko F, Kotschenreuther M and Rogers B N 2000 *Phys. Rev. Lett.* **85** 5579
[15] Dimits A M *et al* 2000 *Phys. Plasmas* **7** 969
[16] Kurihara T *et al* 2000 *Nucl. Instrum. Methods Phys. Res.* B **171** 164
[17] Hugenschmidt C, Kogel G, Schreckenbach K, Sperr P, Strasser B and Triftshauser W 2001 *Mater. Sci. Forum* **363–365** 425
[18] Surko C M, Leventhal M and Passner A 1989 *Phys. Rev. Lett.* **62** 901
[19] Gabrielse G *et al* 1999 *Phys. Lett.* B **455** 311
[20] Greaves R G and Surko C M 2001 *Non-Neutral Plasma Physics IV (AIP Conf. Proc. vol 606)* (New York: American Institute of Physics) p 10
[21] Huba J D 2000 *NRL Plasma Formulary* (Washington, DC: Naval Research Laboratory) p 54 (equation 12)
[22] Gould R J 1989 *Astrophys. J.* **344** 232